

Monoclonal Antibody to ATF6 (Full-length and Active/Cleaved Forms) (Clone 70B1413.1)



11175 Flintkote Ave., Suite E, San Diego, CA 92121
Tel: (858) 642-0978 Fax (858) 642-0937
Toll free: 1-888-723-GENE
E-mail: info@imgenex.com
web site: <http://www.imgenex.com>

Monoclonal Antibody to ATF6 (Full-length and Active/Cleaved Forms) (Clone 70B1413.1)

Catalog No : IMG-273
Formulation : 100 ug in 200 ul PBS containing 0.05% BSA and 0.05% sodium azide. Sodium azide is highly toxic.
Isotype : Mouse IgG1, Kappa
Clone : 70B1413.1
Purification : Protein G Chromatography
Species React : Hamster, Human, Mouse, Rabbit, Rat
Host : Mouse

Application
Western blot analysis: 1-5 ug/ml
IF/ICC: See Thomas et al (2005) and Kikuchi et al (2006) for details.
IHC (paraffin): See van Kollenburg et al (2006) for details.
ChIP: See Donati et al, 2006 and Renna et al, 2007 for details.
IP: See Hong et al, 2004 for details.
IHC (frozen): See Zhu et al, 2008 for details.

Storage
Store at 4°C, stable for 6 months. For long-term storage, aliquot and store at -20°C.

Recommended Positive Control: See Cat No. 40210 [ATF6 transfected cell lysates (transfected & mock transfected)]

Background

ATF6 is a constitutively expressed, endoplasmic reticulum (ER) membrane-anchored transcription factor. ATF6 is a key transcriptional activator of the unfolded protein response (UPR), which allows mammalian cells to maintain cellular homeostasis when they are subjected to environmental and physiological stresses that target the ER (reviewed in Shen and Prywes, and Groenendyk and Michalak). The C-terminus of ATF6 is located in the ER lumen and its N-terminal DNA binding domain faces the cytosol. ATF6 plays a key role in the ER stress response by transmitting the ER stress signal across the ER membrane into the nucleus. The induction of new gene expression by ATF6 is an important aspect of the ER stress response. In response to certain stress conditions, ATF6 translocates from the ER to the Golgi. The 90 kDa full-length ATF6 is processed within the Golgi to its active 50 kDa form through sequential cleavage by site-1 and site-2 proteases (S1P and S2P). Proteolytic activation of ATF6 in the ER stress response is a mechanism to regulate membrane-bound factors, and is referred to as regulated intramembrane proteolysis. The N-terminal active ATF6 translocates to the nucleus where it binds to ER stress-response elements in ER stress-response genes (ERSRGs). ATF6 is a potent transcriptional activator of ESRGs. The fully glycosylated form of ATF6, a 670 amino acid protein, exhibits an electrophoretic mobility of ~90 kDa in denaturing SDS-gels, in part because of the glycosylated modifications. ATF6 has 3 consensus sites for N-linked glycosylation and exists constitutively as a glycosylated protein. Differentially glycosylated ATF6 forms may result from mutations or experimental treatment (Shen and Prywes, 2005).

Antigen

This monoclonal antibody was made against a partial protein containing amino acids 1-273 of human ATF6.

Application Notes

(1) The ATF6 (IMG-273) has been cited to recognize both full-length and cleaved forms of ATF6. Please refer to the references in the Product Citation list for more comprehensive information.

(2) The ATF6 transfected cell lysate (40210) is recommended as a useful western blot positive control to run in parallel with your experimental samples.

(3) Active/cleaved forms of ATF6 are generated through proteolytic cleavage during ER stress. Different molecular weights have been described for cleaved forms. A sample protocol was first described in Luo and Lee (2002) wherein NIH3T3 cells were treated with the amino acid analogue azetidine (AzC), and full-length and cleaved forms ATF6 were detected with IMG-273. The results show that in addition to the major 90 kDa full length ATF6, protein bands over the range of 50-70 kDa were detectable following AzC treatment (Luo and Lee, 2002: Figure 4A, page 791). Many protocols and other cleaved forms have been described since, please consult the literature for additional information.

Monoclonal Antibody to ATF6 (Full-length and Active/Cleaved Forms) (Clone 70B1413.1)

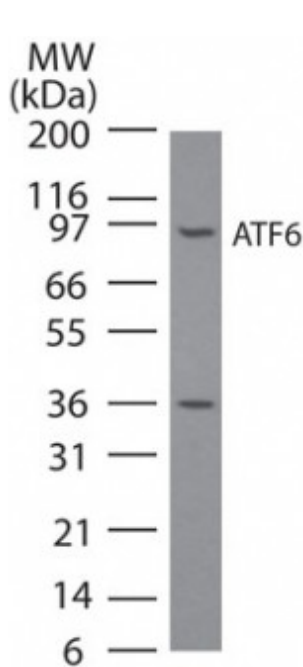
(4) For immunofluorescence microscopy, cells were fixed in methanol at -20 degrees C (Thomas et al, 2005). Thomas et al used immunofluorescence to identify ATF6 with IMG-273 in the nucleus.

(5) The active/cleaved 50 kDa nuclear form of ATF6 using IMG-273 has been found to be strongly expressed in certain tumor cell lines derived from B cell lymphoma (DEL), primary effusion lymphoma [BC-3 (ATCC CRL-2277), PEL-SY, HBL-6], lymphoblastic leukemia (DS-1) and multiple myeloma (RPMI-8226, NCI-H929), (Jenner et al. 2003).

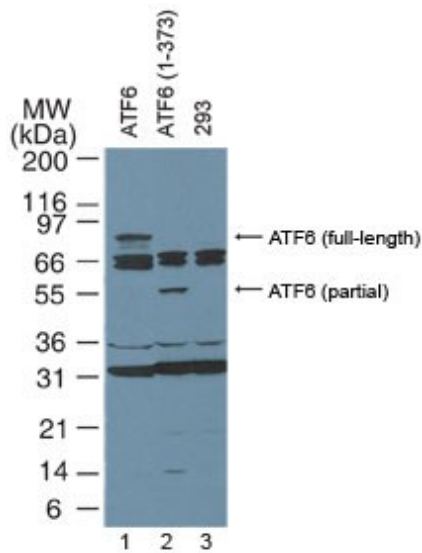
(6) Cleaved 60 and 36 kDa ATF6 forms have also been described in the nucleus (Mao et al, 2007).

(7) The ATF6 antibody is reported to be specific for ATF6 α , recognizing ATF6 α but not ATF6 β (Bommiasamy et al, 2009).

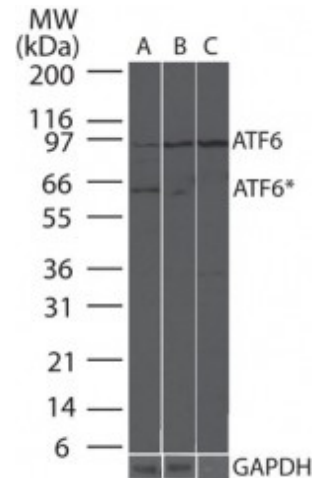
Genebank Info (Protein)
NP_031374



Western blot analysis of ATF6 in NIH3T3 cell lysate using IMG-273 at 3 ug/ml. A band corresponding to full-length ATF6 was detected. We have not characterized the ~36 kDa observed band; it may be an ATF6 breakdown/cleavage product.



Western blot analysis of ATF6. Lane 1, 293 cells transfected with full-length ATF6.* Lane 2, 293 cells transfected with partial length ATF6 (amino acids 1-373).* Lane 3, Untransfected 293 cells. Western blots were probed with 4 ug/ml of the ATF6 monoclonal antibody (IMG-273), followed by an HRP-conjugated second step (20101) and visualized with PicoTect Western Blot Chemiluminescence Substrate (10087K). Film was exposed for 1 min. The top arrow corresponds to the ~90 kDa form of ATF6 described as full-length in the literature.*The human full-length and partial length ATF6 plasmids are described in Luo and Lee (2002).



Western blot analysis of ATF6 in mouse liver tissue enriched using 10088K using 3 ug/ml of IMG-273 (anti-ATF6) and 0.25 ug/ml of IMG-5143A (anti-GAPDH loading control). Lane A contains 20 ugs of whole mouse liver lysate, lane B contains 20 ugs of total ER fraction, and lane C contains 20 ugs of rough ER fraction. The ATF6* band may represent under glycosylated or cleaved/active ATF6.

Monoclonal Antibody to ATF6 (Full-length and Active/Cleaved Forms) (Clone 70B1413.1)

Related Products

- 20101 [Goat Anti-Mouse Ig HRP Conjugate]
- IMG-5019A-1 [Monoclonal Antibody to GAPDH - Loading Control]
- IMG-5019A-2 [Monoclonal Antibody to GAPDH - Loading Control]
- 40210 [Human ATF6 cell lysates (transfected & mock transfected)]
- 40162 [Jurkat cell line lysate (T cell leukemia)]
- 40176 [NIH 3T3 cell line lysate (Swiss albino mouse embryo derived contact-inhibited fibroblast cells)]

Reference

- Groenendyk J and M Michalak. 2005. Endoplasmic reticulum quality control and apoptosis. *Acta Biochimica Polonica* 52:381-295.
- Shen J and R Prywes. 2005. ER stress signaling by regulated proteolysis of ATF6. *Methods* 35:382-389.

Product Citations

- Requirement of the p38 mitogen-activated protein kinase signalling pathway for the induction of the 78kDa glucose-regulated protein/immunoglobulin heavy-chain binding protein by azetidine stress: activating transcription factor 6 as a target for stress-induced phosphorylation. Shengzhan Luo and Amy S. Lee. *Biochem. J.* 366 :787-795 (2002). **IMGENEX antibodies cited: 1. ATF6 (IMG-273) [WB, Fig.4 (NIH3T3 cells)].**
- Kaposi's sarcoma-associated herpesvirus-infected primary effusion lymphoma has a plasma cell gene expression profile. Richard G. Jenner, Karine Maillard, Nicola Cattini, Robin A. Weiss, Chris Boshoff, Richard Wooster, and Paul Kellam. *PNAS* 2003 100: 10399-10404; published online before print as 10.1073/pnas.1630810100. **IMGENEX antibodies cited: 1. ATF6 (IMG-273) [WB, Fig.2 (DLBCL derived DEL cells, PEL cells, and MM-derived cell lines)].**
- Underglycosylation of ATF6 as a Novel Sensing Mechanism for Activation of the Unfolded Protein Response. Min Hong, Shengzhan Luo, Peter Baumeister, Jen-Ming Huang, Raveen K. Gogia, Mingqing Li, and Amy S. Lee. *J. Biol. Chem.* 279: 11354-11363 (2004). **IMGENEX antibodies cited: 1. ATF6 (IMG-273) [WB, Fig.2B (NIH3T3 cells) and Fig.2D (CHO-7 cells)].**
- An SPP reporter activity assay based on the cleavage of type II membrane protein substrates provides further evidence for an inverted orientation of the SPP active site relative to presenilin. Andrew C. Nyborg, Karen Jansen, Thomas B. Ladd, Abdul Fauq, and Todd E. Golde. *J. Biol. Chem.*, 279:43148-42156 (2004). **(Western Blot, Figs 1C, 2C, 2E, 3D: Analysis of a substrate consisting of the N-terminus of ATF6 fused to a transmembrane domain susceptible to SPP cleavage in vitro)**
- 3,3'-Diindolylmethane (DIM) and derivatives induce apoptosis in pancreatic cancer cells through endoplasmic reticulum stress-dependent upregulation of DR5. Abdelrahim M, K Newman, K Vanderlaag, I Samudio, and S Safe. *Carcinogenesis*, Dec 2005; 10.1093/carcin/bgi270. **IMGENEX antibodies cited: 1. ATF6 (IMG-273) 2. DR5 (IMG-120) [WB, Fig.4 and Fig. 6 (Panc-28 cells)].**
- Involvement of a novel Q-SNARE, D12, in quality control of endomembrane system. Okumura A J, K Hatsuzawa, T Tamura, H Nagaya, K Saeki, F Okumura, K Nagao, M Nishikawa, A Yoshimura, and I Wada. *J. Biol. Chem.*, Dec 2005; 10.1074/jbc.M509715200. **IMGENEX antibodies cited: 1. ATF6 (IMG-273) [WB, Fig.5 (NIH3T3 cells)].**
- Cytoprotective gene Bi-1 is required for intrinsic protection from endoplasmic reticulum stress and ischemia-reperfusion injury. Béatrice Bailly-Maitre, Constantino Fondevila, Fady Kaldas, Nathalie Droin, Frédéric Luciano, Jean-Ehrland Ricci, Rhonda Croxton, Maryla Krajewska, Juan M. Zapata, Jerzy W. Kupiec-Weglinski, Douglas Farmer, and John C. Reed. *PNAS*, Feb 2006; 10.1073/pnas.0506854103. **IMGENEX antibodies cited: ATF6 (IMG-273) [WB, Fig 3,5; Supportive Fig 7.11 (Hepatocyte cells)].**
- Nitric oxide induced endoplasmic reticulum stress activates the expression of cargo receptor proteins and alters the glycoprotein transport to the Golgi complex. Renna M, R Faraonio, S Bonatti, D De Stefano, R Carnuccio, G Tajana and P Remondelli., *The International Journal of Biochemistry & Cell Biology*, In Press, (2006) **IMGENEX antibodies cited: 1. ATF6 (IMG-273) [WB, Fig.4 (DETA NONOate- and TG-treated J774 cells)].**
- Endoplasmic Reticulum Stress and Neurodegeneration in Rats Neonatally Infected with Borna Disease Virus. B. L. Williams and W. I. Lipkin. *J. Virol.*, 80: 8613-8626 (2006). **IMGENEX antibodies cited: ATF6 (IMG-273) [WB, Fig 5 (cleaved ATF6 in rat cerebellum and hippocampus tissues)].**
- Flavivirus Infection Activates XBP1 Pathway of the Unfolded Protein Response to Cope with Endoplasmic Reticulum Stress. Yu C-Y, Y-W Hsu, C-L Liao, and Y-L Lin. *J. Virol.*, Sep 2006; 10.1128/JVI.00879-06. **IMGENEX antibodies cited: 1. ATF6 (IMG-273) [WB, Fig.1 (N18 cells)].**
- Acetaminophen induces ER dependent signaling in mouse liver. Nagy G, T Kardon, L Wunderlich, A Szarka, A Kiss, Z Schaff, G Banhegyi, J Mandl. *Archives Biochemistry Biophysics*. Online before print: doi:10.1016/j.abb.2006.11.021. (2007). **IMGENEX antibodies cited: 1. ATF6 (IMG-273) [WB, Fig 5 (full-length and cleaved ATF6 in mouse liver tissue)].**
- Intramembrane proteolytic cleavage by human signal peptide peptidase like 3 and malaria signal peptide peptidase. Nyborg CN, TB Ladd, K Jansen, T Kukar and TE Golde. *FASEB J.* 20:1671-1679 (2006). **IMGENEX antibodies cited: 1. ATF6 (IMG-273) [WB, Fig. 3C: Analysis of a substrate consisting of the N-terminus of ATF6 fused to a transmembrane domain susceptible to SPP cleavage in vitro]**
- Spinal cord endoplasmic reticulum stress associated with a microsomal accumulation of mutant superoxide dismutase-1 in an ALS model. Kukuchi H, G Almer, S Yamashita, C Guegan, M Nagai, Z Xu, AA Sosunov, GM McKhann II and S Przedborski. *PNAS* 103:6025-6030. (2006). **[Western Blots of mouse spinal cord tissue (Fig 1A: full-length and cleaved ATF6) (Fig 6 in supplemental material: cleaved ATF6) (Fig 5C: full-length ATF6 pulled down by immunoprecipitation with a Bip antibody)], IF (mouse spinal cord tissues), Fig 1B.**
- Glia-specific activation of all pathways of the unfolded protein response in vanishing white matter disease. van Kollenburg B, J van Dijk, J Garbern, AAM Thomas, GC Scheper, JM Powers, MS van der Knaap. *J Neuropathol Exp Neurol.*, 65:707-715. (2006). **IMGENEX antibodies cited: 1. ATF6 (IMG-273) [IHC (paraffin), Fig.5A, 5G and 6D (human brain tissue sections)].**
- Reduced cell proliferation and increased apoptosis are significant pathological mechanisms in a murine model of a mild pseudoachondroplasia resulting from a mutation in the C-terminal domain of COMP. Garcia K., R Meadows, L Knowles, D Heinegard, D. Thornton, K Kadler, RP Boot-Hadford, M Briggs. *Hum. Mol. Genet.* 16: 2072-2088 (2007). **WB: Fig 9B, density measurement of Western blots of ATF6 cleavage using tissue from the xiphoid process of mice with pseudoachondroplasia. The authors report a 2.2 increase of cleaved ATF6 in mutant compared to normal chondrocytes.**
- Cadiomyocyte apoptosis in autoimmune cardiomyopathy: mediated via endoplasmic reticulum stress and egerated by norepinephrine. Mao W, S fukuoka, C Iwai, J Liu, VK Sharma, S-S Sheu, M Fu, and C-s Liang. *Am J Heart Circ Physiol* 293:H1636-H1645 (2007). **Imgenex antibodies cited: 1. ATF6 (IMG-273): WB (Fig 7), analysis of ATF6 in nuclear fraction of rabbit left ventricle myocardium tissue lysates, Authors describe cleaved forms of p90ATF6 in the nucleus: the cleaved forms are described as p60ATF6 and p36ATF6.**
- GAPDH (IMG-5019A): WB (Fig 4), GAPDH antibody used as a loading control in rabbit left ventricle myocardium tissue lysates.
- Carbon monoxide induces heme oxygenase-1 via activation of protein kinase R-like endoplasmic reticulum kinase and inhibits endothelial cell apoptosis triggered by endoplasmic reticulum stress. Kim KM, H-O Pae, M Chung, R Park, Y-M Kim, H-T Chung. *Circulation Research* DOI: 10.1161/CIRCRESAHA.107.154781. (2007). **WB (Figs 3, 4, 6): HUVEC (human umbilical vein endothelial cells), p90ATF6 and cleaved p50ATF6 forms of ATF6 are detected.**
- The kinase inhibitor sorafenib induces cell death through a process involving induction of endoplasmic reticulum stress. Rahmani M, EM Davis, TR Crabtree, JR Habibi, TK Nguyen, P Dent and S Grant. *Molecular and Cellular Biol.* 27:5499-5513 (2007). **WB: Fig 3A, U937 human leukemia cells treated with sorafenib. Sorafenib is a multikinase inhibitor that induces apoptosis in human leukemia and other malignant cells. The authors show a decline in ATF6 (90 kDa band) expression in sorafenib-treated cells.**
- Effects of triglyceride on ER stress and insulin resistance. Kim D-S, S-K Jeong, H-R Kim, D-S kim, S-W Chae, and H-J Chae. *Biochem. Biophys. Res. Comm.* doi:10.1016/j.bbrc.2007.08.151 (2007). **WB (Fig 2), HepG2 cells treated with triglyceride. There was an increase of cleaved ATF6 over time with the triglyceride treatment.**
- GM1-Ganglioside-mediated activation of the unfolded protein response causes neuronal death in a neurodegenerative gangliosidosis. Tessitore A, MDP Martin, R Sano, Y Ma, L Mann., A Ingrassia, ED Laywell, DA Steindler, LM Hendershot, and A d'Azzo. *Molecular Cell* 15:753-766 (2004). **WB: Fig 7A, mice spinal cord tissue. Lysosomal B-galactosidase -/- mice had increased levels of the 50 kDa cleaved form of ATF6 compared to wild-type mice.**
- Endoplasmic reticulum stress contributes of beta cell apoptosis in type 2 diabetes. Laybutt DR, AM Preston, MC Akerfeldt, JG Kench, AK Busch, AV Biankin, and TJ Biden. *Diabetologia* 50:752-763. **WB (Fig 3a and c), MIN6 mouse cells treated with DDIT3 (DNA-damage inducible transcript 3). MIN6 is a pancreatic beta cell line that retains glucose-inducible insulin secretion. The results showed an increase in the cleaved 50 kDa form of ATF6 at certain time points in DDIT3-treated compared to BSA-treated control cells.**
- Dynamic recruitment of transcription factors and epigenetic changes on the ER stress response gene promoters. Donati G, C Imbriano, and R Mantovani. *Nucleic Acids Research* 34:3116-3127 (2006). **ChIP (Fig 5), HepG2 cells treated with thapsigargin.**
- Effect on tumor cells of blocking survival response to glucose deprivation. Park H-R, A Tomida, S Sato, Y Tsukumo, J Yun, T Yamori, Y Hayakawa, T Tsuruo, K Shin-ya. *J National Cancer Institute* 96:1300-1310 (2004). **WB (HT1080 human fibrosarcoma cells): Fig 2a. HT1080 cells transfected with full-length ATF6(F) or active ATF6(A) and treated with 2-deoxyglucose (2DG) or tunicamycin (TM) in the presence or absence of versipelostatatin (VST). ATF(F), un/under-glycosylated ATF6, intermediate ATF6 and ATF6 (A) forms are detected. Fig 2d. HT1080 cells transfected with ATF6 (A) and treated with 2DG in the presence or absence of VST. ATF6 (A) is shown, VST did not inhibit the production of ATF6 (A). Fig 4e. ATF6 (F) and mock-transfected HT1080 cells. ATF6(F) is shown; ATF6-transfected cells had a higher expression level of ATF6 (F) than the exogenous level seen in mock-transfected cells. Furthermore, the level of ATF6 (F) increased with increasing amounts (1 to 100 ng) of the ATF6 (F) plasmid used for transfection.**

ATF6 Transfection Validated: The ATF6 (IMG-273) antibody is validated by transfection to recognize ATF6 (F), un/under-glycosylated ATF6, intermediate ATF6 and ATF6 (A) forms in this citation (Figs 2a, 2d and 4e).

- Regulation of ERGIC-53 gene transcription in response to endoplasmic reticulum stress. Renna M, MG Caporaso, S Bonatti, RJ Kaufman, and P Remondelli. *JBC*

Monoclonal Antibody to ATF6 (Full-length and Active/Cleaved Forms) (Clone 70B1413.1)

- 282:22499-22512 (2007). ChIP: Fig 6B, Steady-state and thapsigargin (Tg)-treated HeLa cells. BiP/Grp78 and ERGIC-53 promoter regions were used as PCR primers in the ChIP assays to assess DNA ATF6 protein interactions. In Tg-treated cells there was endogenous ATF6 binding on both the promoter regions.
25. Heat shock protein inhibition is associated with activation of the unfolded protein response pathway in myeloma plasma cells. Davenport EL, HE Moore, AS Dunlop, SY Sharp, P Workman, GJ Morgan and FE Davies. *Blood* 100:2641-2649 (2007). **WB** (analysis of cleaved ATF6 nuclear fractions of human myeloma cells (U266, H929, MMJ) treated with tunicamycin, thapsigargin, HSP inhibitors, or bortezomib): Figs 1C, 2C, and 3C. Results show increase of cleaved ATF6 under certain treatment conditions.
26. Bax inhibitor-1 regulates endoplasmic reticulum stress-associated reactive oxygen species and heme oxygenase-1 expression. Lee G-H, H-K Kim, S-W Chae, D-S Kim, K-C Ha, M Cuddy, C Kress, JC Reed, H-R Kim, and J-J Chae. *JBC* 282:21618-21628 (2007). **WB**: Neo and BI-1 transfected human HT1080 fibrosarcoma cells treated with thapsigargin or tunicamycin (analysis of uncleaved ATF6 (p90)), Fig. 3A-C. The results showed that the level of uncleaved ATF6 (p90) was lower in Neo than in BI-1 cells. They also that the basal level of ATF6 (p90) decreased in Neo cells under ER stress but remained unchanged in the BI-1 cells under ER stress.
27. Nitric oxide induces coupling of mitochondrial signalling with the endoplasmic reticulum stress response. Weiming X, L Liu, IG Charles, and S Moncada. *Nature Cell Biology* 6:1129-1134 (2004). **WB** (analysis of p90 and p50 ATF6): Tex293 and EcR293 cells treated with various agents, Figs 1d, 2a, and 3b. Collectively the results show an increase of p50 ATF6 under certain treatment conditions.
28. Long QT syndrome-associated I593R mutation in HERG potassium channel activates ER stress pathways. Keller SH, O Platoshyn, and J X-J Yuan. *Cell Biochemistry and Biophysics* 43:365-377. **WB** (analysis of full-length and active ATF6) and **IP**: HEK-293 and HeLa cells transfected with WT/WT HERG, WT/1593 HERG or 1593/1593 HERG, Fig 6B: WB with ATF6, showing increase of active (50 kDa ATF6) in WT/1593 and 1593/1593 HERG compared to WT/WT cells) Fig 6C: IP with ATF6 and WB with Grp78, showing increase of Grp78 in WT/1593 and 1593/1593 HERG compared to WT/WT cells; IP/WB with ATF6 (similar results, data described but not shown)
29. ER and oxidative stresses are common mediators of apoptosis in both neurodegenerative and non-neurodegenerative lysosomal storage disorders and are alleviated by chemical chaperones. Wei H, S Kim, Z Zhang, P Tsai K Wisniewski, A Mukherjee. *Human Molecular Genetics* 17: 469-477 (2008). **WB** (human LSD (lysosomal storage disease) and normal cell lines), Figs. 1A,C; 3A,B,C.
30. Shiga toxin 1 induces apoptosis through the endoplasmic reticulum stress response in human monocytic cells. Lee S, M Lee, R Cherala, V Tesh. *Cellular Microbiology* 10:770-780 (2008). **WB** (human myelogenous leukemia cell line THP-1 cells), Fig. 1A. **Note**: The degradation of the 90 kDa ATF6 band was detected in THP-1 cells treated with Stx1. As shown in Fig 1A the levels of immunoreactive 90 kDa ATF6 were decreased beginning 2 h after Stx1 treatment and remained decreased over the time-course of the experiment. The Stx1 mutant failed to initiate the degradation of 90 kDa ATF6. The degradation of the 90 kDa band is considered to be an indication of ATF6 activation.
31. Eif-2a protects brainstem motoneurons in a murine model of sleep apnea. Zhu Y, P Fenik, G Zhan, B Sanfilippo-Cohn, N Naidoo, and SC Veasey. *J Neuroscience* 28:2168-2178. **Mouse brain**: IHC (frozen), Fig 2B; WB, Fig 1B. See Table I for information on antibody concentrations used. Immunofluorescence was used as a detection method for the IHC (frozen) images.
32. HMG-CoA reductase inhibitors activate the unfolded protein response and induce cytoprotective GRP78 expression. J Chen, M Wu, K Huang, W Lin. *Cardiovascular Research* 80: 138-150 (2008). **WB** (mouse RAW 264.7 cells), Fig. 5C.
33. cAbi kinase inhibitors overcome CD40-mediated drug resistance in CLL; Implications for therapeutic targeting of chemoresistant niches. *Blood* doi:10.1182/blood-2008-03-146704 (2008). **WB** (human chronic lymphocytic leukemia cells), Supplementary Fig. 1a,b.
34. Chemical biology investigation of cell death pathways activated by endoplasmic reticulum stress reveals cytoprotective modulators of ASK1. Kim I, C Shu, W Xu, C Shiau, D Grant, S Vasile, N Cosford, J Reed. *J Biol. Chem* 283: 1593-1603 (2009). **WB** (human CSM14.1 cells), Fig. 3.
35. ATF6 α induces XBP1-independent expansion of endoplasmic reticulum. Bommasamy H, SH Back, P Fagone, K Lee, S Meshinchi, E Vink, R Sruburi, M Frank, S Jackowski, RJ Kaufman, and JW Brewer. *J Cell Sci* 122:1626-1636 (2009). **WB**: ATF6 transfected CHO cells (Fig 2). The antibody detected ATF6 α but not ATF6 β transfected cells, thereby showing that the antibody specifically recognized the ATF6 α isoform. **Note**: The antibody was transfected ATF6 α validated by WB in Fig 2.
36. The unfolded protein response modulates toxicity of the expanded glutamine androgen receptor. Monzy Thomas, Zhigang Yu, Nahid Dadgar, Sooryanarayana Varambally, Jianjun Yu, Arul M. Chinnaiyan, and Andrew P. Lieberman. *J. Biol. Chem.*, 280: 21264-21271 (2005). **IMGEX antibodies cited: ATF6 (IMG-273) [IF/ICC, Fig 2A (Quantification of nuclear active ATF6)]**.
37. Endoplasmic reticulum stress triggers an acute proteasome-dependent degradation of ATF6. Hong M, L Mingqing, C Mao, and AS Lee. *J Cellular Biochemistry* 92:723-732 (2004). **WB**:
(1) NIH3T3 cells:
Fig 1C: Thapsigargin (Tg) treatment. At 0 hr, p90ATF6 was present at a low basal level. Treatment resulted in the transient disappearance of p90ATF6 at 2 hr. By 8 hrs of treatment, ATF6 was elevated.
Fig 1D: Tunicamycin treatment At 0 hr, p90ATF6 was present at a low basal level. Treatment resulted in the disappearance of p90ATF6. At 8 hr a faster-migrating ATF6 band appeared, referred to as the non-glycosylated form of ATF6.
Fig 3A: Tg treatment and pretreatment with either ALLN, MG115 or z-DEVD-FMK. Pretreatment with ALLN or MG115 partially rescued Tg-induced ATF6 degradation at 2 hr. z-DEVD-FMK did not prevent ATF6 degradation at 2 hr.
Fig 3B: Treated with calpastatin peptide C1, Tg or peptide + Tg. Treatment with the peptide did not prevent ATF6 degradation at 2 hr. + Tg or Tg alone NIH3T3 This was transient and by 8 hr of Tg treatment, ATF6 was elevated.
Treatment diminished the level of p90ATF6.
Figs 4A and 4B: Treated with with combinations Tg, MG115, and ALLN. Treatment with MG115, but not ALLN resulted in a slight increase in the steady state level of p90ATF6.
- 2 (CHO cells):
Figs 2A-D: Various CHO constructs treated with Tg. Collectively the results show that both endogenous and ectopic p90ATF6 were subjected to acute proteolysis immediately following Tg stress.
- IP/WB** (NIH3T3 cells)
Fig 3C: Treated with Tg in the presence of MG132, IP with ATF6 antibody, WB with Ubiquitin antibody (top) or IP/WB with ATF6 antibody. Results show that in non-stressed cells, ubiquitinated p90ATF6 was present and that ubiquitination increased substantially within 1-2 h of Tg treatment. **Thus in non-stressed cells, p90ATF6 is subjected to constitutive proteasome-ubiquitin degradation.**
38. Intrinsic capacities of molecular sensors of the unfolded protein response to sense alternate forms of endoplasmic reticulum stress. DuRose JB, AB Tam and M Niwa. *Mol Biol Cell*, 17:3095-3017 (2006). **IMGEX antibodies cited: 1. ATF6 (IMG-273) [WB, Fig 1: full-length and cleaved ATF6 in CHO cells] , [WB, Fig 2 (full-length ATF6 in HeLa cells)]**.

Copyright © IMGEX Corporation. All Rights Reserved

Toll free: 1-888-723-4363

Fax: 1-858-642-0937

www.imgenex.com

info@imgenex.com

Research purposes only. Not for diagnostic or in vivo use.